IEEE Photonics Journal
An IEEE Photonics Society Publication

Open Access

Triangular Microwave Waveform Generation Based on Stimulated Brillouin Scattering

Volume 6, Number 6, December 2014

Wen Hui Sun
Wei Li
Wen Ting Wang
Wei Yu Wang
Jian Guo Liu
Ning Hua Zhu

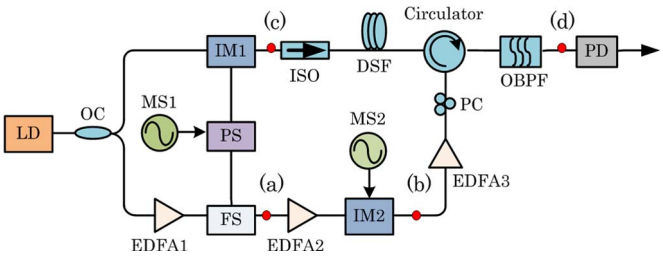

DOI: 10.1109/JPHOT.2014.2361606
1943-0655

Triangular Microwave Waveform Generation Based on Stimulated Brillouin Scattering

Wen Hui Sun, Wei Li, Wen Ting Wang, Wei Yu Wang, Jian Guo Liu, and Ning Hua Zhu

State Key Laboratory on Integrated Optoelectronics, Institute of Semiconductors, Chinese Academy of Sciences, Beijing 100083, China

DOI: 10.1109/JPHOT.2014.2361606

Manuscript received August 27, 2014; revised September 25, 2014; accepted September 26, 2014. Date of publication October 15, 2014; date of current version November 24, 2014. This work was supported by the National Natural Science Foundation of China under Grant 61377069, Grant 61335005, Grant 61321063, and Grant 61090391. Corresponding author: W. Li (e-mail: liwei05@semi.ac.cn).

Abstract: We proposed a new approach to generate full-duty-cycle triangular waveforms using a sinusoidal radio-frequency (RF) signal based on stimulated Brillouin scattering. In order to generate a triangular waveform, the even-order harmonics of the RF signal has to be removed. In our scheme, we use both the pump and Stokes waves to manipulate the amplitudes and phases of the optical components. In this way, the amplitudes and phases of the fundamental RF tone and its harmonics can be controlled. The proposed method is theoretically analyzed and experimentally verified. For a proof-of-concept demonstration, triangular waveforms at 8.5, 10.5, and 12.5 GHz are generated. The measured results agree well with the simulated ones.

Index Terms: Microwave photonics, triangular waveforms, stimulated Brillouin scattering (SBS).

1. Introduction

The generation of microwave arbitrary waveforms has attracted much attention for its widespread applications, such as all-optical microwave signal processing, modern radar systems, electronic test and measurement, and wired and wireless communications [1]–[4]. Many approaches have been proposed to generate microwave waveforms. The desired microwave waveforms can be generated based on optical spectrum shaping and frequency-to-time mapping [5], [6]. Generally, the optical spectrum of a mode locked laser is tailored by an optical spectrum shaper. A dispersive element is used to realize frequency-to-time mapping. After photodetection, a microwave waveform with a scaled version of the tailored optical spectrum is generated [5]. However, the triangular pulses generated using an ultra-short optical pulse have small duty cycle (< 1). For many applications, triangular waveforms with full-duty-cycle are highly desired. For example, full-duty-cycle triangular waveforms have been used to doubling the optical signals [7].

Microwave waveforms can also be generated using sinusoidal microwave signal and external modulation. In these schemes, triangular waveforms with full-duty-cycle $(= 1)$ can be generated. In [8], a microwave waveform generator using a polarization modulator (PolM) in a Sagnac loop is proposed. By tuning the polarization controller and the power of the sinusoidal microwave signal, triangular waveforms were successfully generated. Triangular-shaped microwave pulses

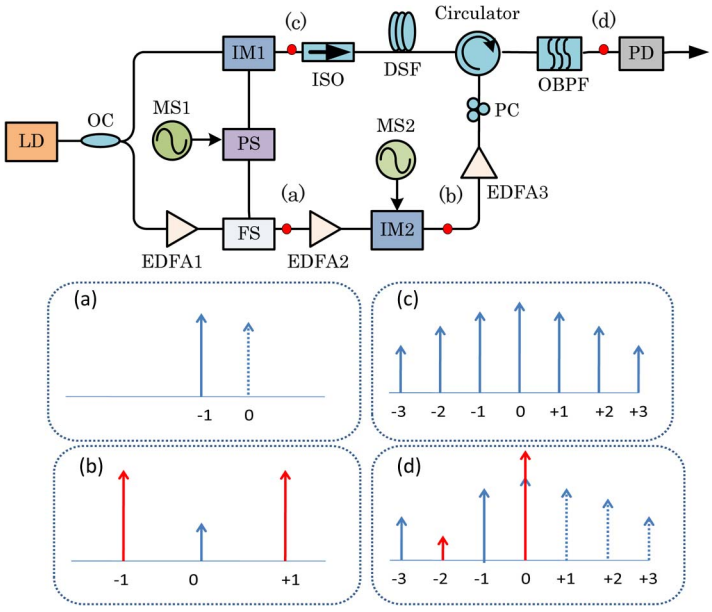

Fig. 1. Schematic diagram of the proposed triangular waveform generator. LD: laser diode, OC: optical coupler, MS1: microwave source 1, MS2: microwave source 2, PS: power splitter, IM1: intensity modulator 1, IM2: intensity modulator 2, ISO: optical isolator, OBPF: optical bandpass filter, EDFA: erbium-doped fiber amplifier, PC: polarization controller, PD: photodetector.

with tunable repetition rate were generated using a Mach–Zehnder modulator (MZM) and an interleaver [9]. By properly setting the bias voltages of a dual-parallel Mach–Zehnder modulator (DPMZM), a full-duty-cycle triangular waveform was generated [10], [11].

Recently, we have demonstrated the generation of triangular waveforms using microwave photonics filter with negative coefficient [12] and nonlinear polarization rotation in a highly nonlinear fiber [13]. Generation of triangular waveform has also been reported using other nonlinear effect in optical fiber. In [14], triangular microwave waveform has been generated using stimulated Brillouin scattering (SBS) in optical fiber and MZM. In this method, the MZM was biased at the null point to suppress the optical carrier and even-order optical sidebands. The residual optical carrier was amplified by a pump signal via SBS effect in order to generate a triangular waveform. However, it should be noted that the optical carrier would be fully suppressed for an ideal MZM and could not be amplified via the SBS process. This method can only work for an imperfect MZM where the optical carrier is not fully eliminated by setting the bias at the null point.

In this paper, we propose a new method to generate full-duty-cycle triangular waveform using SBS in optical fiber. Different from the previous method [14], our scheme is independent on the performance of the MZM, which is more practical for a real application. In our scheme, both the SBS amplification and attenuation are used to process the optical carrier and modulation sidebands. The amplitude and phase of the optical carrier are manipulated using a pump wave, while the second-order optical sideband is suppressed by a Stokes wave. After photodetection, triangular waveforms are generated. The proposed method has been theoretically analyzed and experimentally verified. Triangular waveforms at 8.5, 10.5, and 12.5 GHz have been successfully generated. In addition, the simulated results fit well with the measured ones.

2. Operational Principle

The schematic diagram of the triangular waveform generator is shown in Fig. 1. An optical carrier from a laser diode (LD) is splitting into two parts by a 3-dB optical coupler. The upper part is sent to IM1 which is driven by a sinusoidal microwave signal. It is worth noting that the MZM is

biased at quadrature point in our scheme rather than the null point as reported in [14]. The schematic optical spectrum is shown in Fig. 1(b). An optical isolator (ISO) was used to realize unidirectional optical transmission. The optical signal at the output of the ISO is sent to an optical circulator (port 2) through a spool of dispersion-shifted fiber (DSF).

For the lower part optical carrier, it is first red-shifted by a frequency shifter (FS) [15], as shown in Fig. 1(a). The FS is also driven by the microwave signal from MS1. Afterward, the red-shifted optical signal is modulated by the other IM2 which is driven by a microwave signal with the frequency of ω_{m2}. IM2 is biased at the null point to generate a carrier-suppressed double-sideband (CS-DSB) modulated optical signal, as shown in Fig. 1(b). Polarization Controller (PC) was used to align the polarization state of the pump light and stokes light. The lower-frequency and upper-frequency optical sidebands act as the pump and Stokes waves, respectively, to stimulate the SBS effect in the DSF. As a result, the amplitude of the optical carrier at the upper part is amplified by the pump wave. Moreover, its phase can also be tuned over 360° via SBS effect [16]–[18]. On the other hand, the amplitude of the second-order optical sideband at higher frequency side is attenuated by the Stokes wave. An optical bandpass filter (OBPF) is attached at the port 3 of the optical circulator to remove the undesired optical sideband at lower frequency side. After detecting by a photodetector (PD), triangular microwave waveforms can be generated.

A triangular waveform can be expressed by the Fourier series [14]

$$T(t) = A + \sum_{m=1,3,5}^{\infty} \frac{1}{m^2} \cos[m(\omega_m t + \varphi)] \tag{1}$$

where φ is the initial phase of the fundamental sinusoidal microwave signal. As can be seen from (1), the triangular waveform consists of only odd-order harmonics. In our scheme, the even-order harmonics are eliminated by manipulating the optical components of the optical signal. For the upper part, the optical field at the output of the IM1 can be expressed as

$$E_1(t) = \frac{1}{2} \exp(j\omega_0 t)\{\exp[j\beta\cos(\omega_{m1} t) + j\varphi] + \exp[-j\beta\cos(\omega_{m1} t)]\} \tag{2}$$

where $\beta = \pi V_m / V_\pi$ is the modulation index of the IM1, and V_m and V_π are the amplitude of the microwave signal and the half-wave voltage of the IM1, respectively. $\varphi = \pi V_{Bias} / V_\pi$ is the phase shift between the two arms of the IM1, which is controlled by the bias V_{Bias} of the IM1. Applying Jacobi Anger expansion to (2), we have

$$E_1(t) = \frac{1}{2} \exp(j\omega_0 t) \left\{ \sum_{n=-\infty}^{\infty} j^n J_n \exp(jn\omega_m t + j\varphi)] + \sum_{n=-\infty}^{\infty} (-j)^n J_n \exp(jn\omega_m t) \right\} \tag{3}$$

where $J_n = J_n(\beta)$ is the Bessel function for the first kind of order n.

For the lower part in our scheme, the optical field at the output of the FS is given by $E_{fs}(t) = \exp[j(\omega_0 - \omega_{m1})t]$. This red-shifted optical signal is modulated by IM2, i.e.,

$$E_p(t) = E_p \exp[j(\omega_0 - \omega_{m1} + \omega_{m2})t] \tag{4a}$$

$$E_S(t) = E_S \exp[j(\omega_0 - \omega_{m1} - \omega_{m2})t] \tag{4b}$$

where ω_0 is the angular frequency of the optical carrier, ω_{m1} is the angular frequency of the sinusoidal microwave signal from MS1, and the frequency of the sinusoidal microwave signal fed to the IM2 is $\omega_{m2} = (\omega_{m1} + \omega_B)$, $\omega_B = 2\pi V_B$ is the angular frequency of Brillouin frequency shift.

In the DSF, the signal wave interacts with the pump and Stokes waves, as shown in Fig. 2. Afterward, an OBPF is used to remove the optical sidebands at the lower frequency side. The

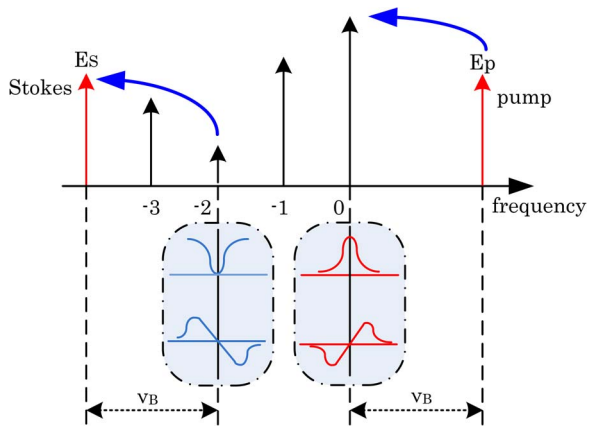

Fig. 2. Operational principle for suppressing the second-order sideband and amplifying the optical carrier based on SBS.

resulted optical field is given by

$$E_2(t) = \exp(j\omega_0 t)\Big\{\sqrt{G}J_0\exp(j\phi_1) + J_{-1}\exp(-j\omega_m t) + \sqrt{L}J_{-2}\exp(-j2\omega_m t + j\phi_2 + j\pi) + J_{-3}\exp(-j3\omega_m t + j\pi)\Big\} \quad (5)$$

where ϕ_1, ϕ_2 are phase shifts introduced by the SBS to the optical carrier and the second-order sideband. G and L are the gain and loss coefficients of the SBS process. The PD is used to convert the optical signal to electrical signal. As the second-order optical sideband is significantly attenuated by the Stokes wave, it is neglected in the following analysis. The photocurrent at the output of the PD can be expressed as

$$i \propto DC + \sqrt{G}J_0J_1\cos(\omega_m t - \phi_1) + J_1J_3\cos(2\omega_m t) + \sqrt{G}J_0J_3\cos(3\omega_m t - \phi_1 - \pi). \quad (6)$$

If the gain of the SBS is large enough, we have

$$\sqrt{G}J_0J_3 \gg J_1J_3. \quad (7)$$

Therefore, the second harmonic in (6) can be ignored. Comparing (6) with (1), the following conditions have to be satisfied to generate a triangular waveform

$$J_3/J_1 = 1/9, \quad (8a)$$

$$\phi_1 = \pi/2. \quad (8b)$$

In order to satisfy the condition of $J_3/J_1 = 1/9$, we have $\beta = 1.51$. Thus, (6) can be simplified as

$$i \propto DC + \cos\left(\omega_m t - \frac{\pi}{2}\right) + \frac{1}{9}\cos\left(3\omega_m t - \frac{3\pi}{2}\right). \quad (9)$$

It can be seen from (9) that the generated microwave signal is a triangular waveform. It is noted that the repetition rate of the triangular waveform can be adjusted by simultaneously tuning the frequency of the MS1 and MS2 but keeping their frequency difference V_B unchanged.

3. Experiments and Results

We carried out experiments based on the configuration shown in Fig. 1 to verify the feasibility of the proposed approach. An optical carrier at 1550 nm from a laser diode (LD) was sent to a 3-dB OC. For the lower part, the optical signal is red-shifted by 10 GHz via a FS.

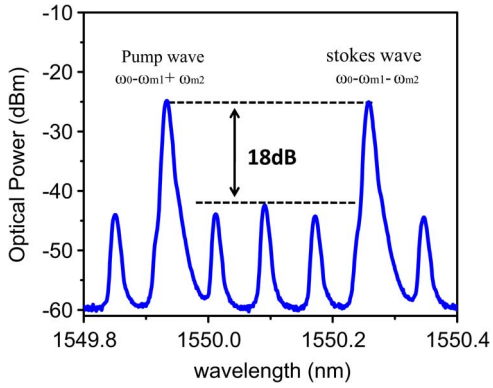

Fig. 3. Measured optical spectrum at the output of the IM2. $\omega_{m1} = 10$ GHz, and $\omega_{m2} = 20.54$ GHz.

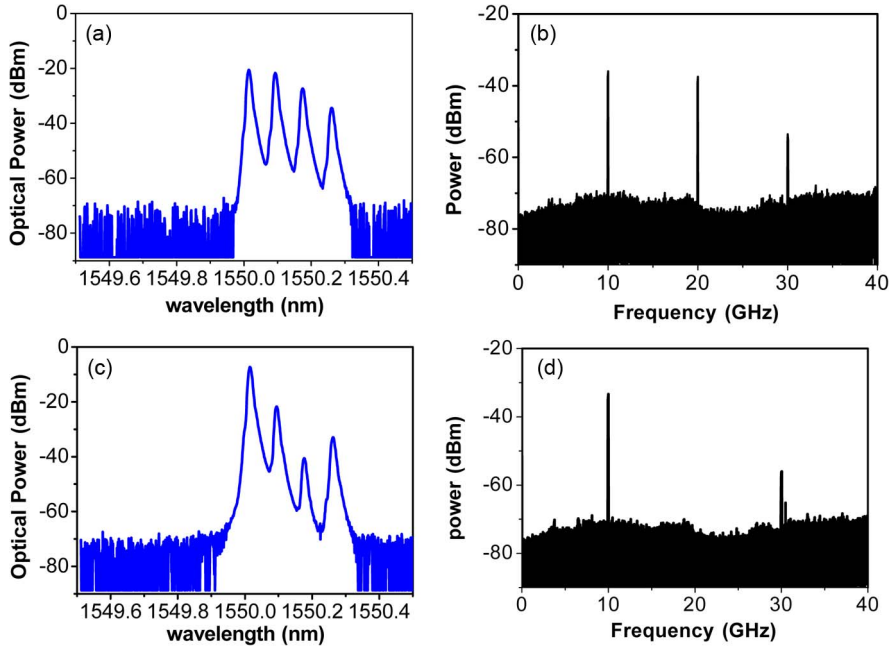

Fig. 4. Measured optical spectra at the output of the OBPF (a) without and (c) with SBS. Measured electrical spectra at the output of the OBPF (b) without and (d) with SBS.

The red-shifted optical signal was then CS-DSB modulated by IM2. The frequency of the microwave signal was 20.54 GHz. It is noted that Brillouin frequency shift V_B of the 4.1 km DSF used in our experiment is around 10.54 GHz. The measured optical spectrum at the output of the IM2 is shown in Fig. 3. The undesired optical components are 18 dB lower than the desired one. The undesired optical components were generated due to the limited extinction ratio of the FS and MZM.

For the upper part, the optical carrier was modulated by the IM1 which is biased at the quadrature point. The frequency of the microwave signal driven to the IM1 is 10 GHz. Polarization Controller (PC) was used to align the polarization state of the pump light and stokes light. The measured optical spectrum at the output of the OBPF without SBS interaction is shown in Fig. 4(a). It mainly consists of an optical carrier, first-order sideband, second-order sideband, and third-order sideband. The corresponding electrical spectrum is shown in Fig. 4(b). It can be seen that there is a large second-order harmonics due to the beat between the optical carrier and second-order sideband as well as that between the first-order and the third-order

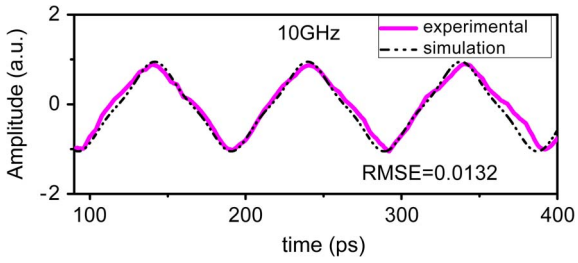

Fig. 5. Measured and simulated triangular waveforms at the repetition rate of 10 GHz.

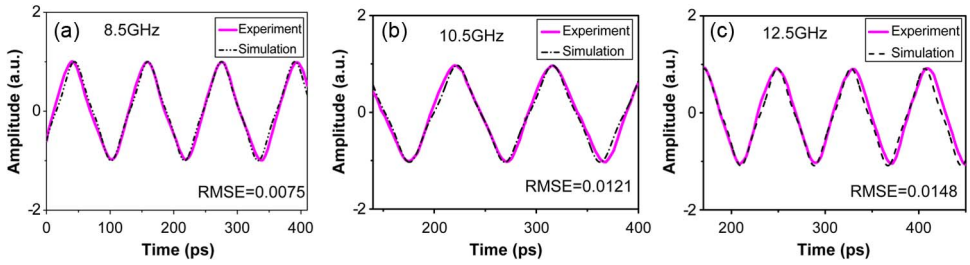

Fig. 6. Triangular waveforms with tunable repetition rate at (a) 8.5 GHz, (b) 10.5 GHz, and (c) 12.5 GHz.

sidebands. When the SBS process was involved, the amplitude and phase of the optical carrier and the second-order sideband are modified. The resulted optical spectrum is shown in Fig. 4(c). As can be seen, the optical carrier is amplified while the second-order sideband is attenuated. The measured electrical spectrum is shown in Fig. 4(d). The second-order harmonic is well suppressed. The third-order harmonic is 20.84 dB lower than the fundamental tone. The signal-to-noise ratios of the fundamental tone and the third-order harmonics are 43 dB and 20 dB, respectively. This suppression ratio is very close to the ideal one of 19.08 dB. The measured and simulated waveforms of the microwave signal is shown in Fig. 5. A triangular waveform with full-duty-cycle at 10 GHz is generated. The simulated waveform matches well with the measured one. The root-mean-square error (RMSE) is calculated to be 0.0132.

To show the tunability of the proposed triangular waveform generator, we also generated triangular waveforms at other repetition rates. Fig. 6 shows the generated triangular waveforms at 8.5, 10.5, and 12.5 GHz. The RMSEs between simulated and the measured results are 0.0075, 0.0121, and 0.0148 for triangular waveforms at 8.5, 10.5, and 12.5 GHz, respectively. The RMSEs between the simulated and the ideal results can be found elsewhere [8].

4. Conclusion

In conclusion, we have theoretically and experimentally demonstrated a new method to generate triangular waveform based on SBS. Both the Brillouin amplification and attenuation have been used to manipulate the amplitude and phase of the modulated optical components. By properly adjusting the power of the sinusoidal microwave signal as well as the pump and Stokes waves involved in the SBS process, triangular waveforms can be generated. For a proof-of-concept demonstration, triangular waveforms at 8.5 GHz, 10.5 GHz, and 12.5 GHz have been generated. The measured and simulated results agree well with each other.

References

[1] F. Parmigiani *et al.*, "Efficient optical wavelength conversion using triangular pulses generated using a superstructured fiber Bragg grating," in *Proc. OFC*, San Diego, CA, USA, pp. 1–3, paper OMP3.
[2] A. W. Rihaczek, *Principles of High-Resolution Radar*. Norwood, MA, USA: Artech House, 1996.

[3] J. P. Yao, "Photonic generation of microwave arbitrary waveforms," *Opt. Commun.*, vol. 284, no. 15, pp. 3723–3736, Jul. 2011.
[4] R. S. Bhamber, A. I. Latkin, S. Boscolo, and S. K. Turitsyn, "All-optical TDM to WDM signal conversion and partial regeneration using XPM with triangular pulses," in *Proc. 34th ECOC*, Brussels, Belgium, 2008, pp. 1–2.
[5] J. Ye, L. S. Yan, W. Pan, B. Luo, X. H. Zou, A. L. Yi, and S. Yao, "Photonic generation of triangular-shaped pulses based on frequency to time conversion," *Opt. Lett.*, vol. 36, no. 8, pp. 1458–1460, Apr. 2011.
[6] C. B. Huang, D. E. Leaird, and A. M. Weiner, "Time-multiplexed photonically enabled radio-frequency arbitrary waveform generation with 100 ps transitions," *Opt. Lett.*, vol. 32, no. 22, pp. 3242–3244, Nov. 2007.
[7] A. I. Latkin, S. Boscolo, R. S. Bhamber, and S. K. Turitsyn, "Doubling of optical signals using triangular pulses," *J. Opt. Soc. Amer. B*, vol. 26, no. 8, pp. 1492–1496, Aug. 2009.
[8] W. Liu and J. P. Yao, "Photonic generation of microwave waveforms based on a polarization modulator in a Sagnac loop," *J. Lightw. Technol.*, vol. 32, no. 20, pp. 3637–3644, Oct. 2014.
[9] J. Li, T. Ning, L. Pei, W. Jian, H. You, H. Chen, and C. Zhang, "Photonic-assisted periodic triangular-shaped pulses generation with tunable repetition rate," *IEEE Photon. Technol. Lett.*, vol. 25, no. 10, pp. 952–954, May 2013.
[10] F. Zhang, X. Ge, and S. Pan, "Triangular pulse generation using a dual-parallel Mach–Zehnder modulator driven by a single-frequency radio frequency signal," *Opt. Lett.*, vol. 38, no. 21, pp. 4491–4493, Nov. 2013.
[11] W. Li, W. T. Wang, and N. H. Zhu, "Photonic generation of radio-frequency waveforms based on dual-parallel Mach–Zehnder modulator," *IEEE Photon. J.*, vol. 6, no. 3, Jun. 2014, Art. ID. 5500608.
[12] W. Li, W. T. Wang, W. H. Sun, W. Y. Wang, and N. H. Zhu, "Generation of triangular waveforms based on a microwave photonic filter with negative coefficient," *Opt. Exp.*, vol. 22, no. 12, pp. 14 993–15 001, Jun. 2014.
[13] W. Li, W. Y. Wang, W. H. Sun, W. T. Wang, J. G. Liu, and N. H. Zhu , "Photonic generation of triangular pulses based on nonlinear polarization rotation in a highly nonlinear fiber," *Opt. Lett.*, vol. 39, no. 16, pp. 4758–4761, Aug. 15, 2014.
[14] X. Liu, W. Pan, X. Zou, D. Zheng, L. Yan, B. Lou, and B. Lu, "Photonic generation of triangular-shaped microwave pulses using SBS-based optical carrier processing," *J. Lightw. Technol.*, vol. 32, no. 20, pp. 3797–3802, Oct. 15, 2014.
[15] M. Izutsu, T. Sueta, and S. Shikama, "Integrated optical SSB modulator/frequency shifter," *IEEE J. Quantum. Electron.*, vol. QE-17, no. 11, pp. 2225–2227, Nov. 1981.
[16] A. Loayssa, D. Benito, and M. J. Garde, "Applications of optical carrier Brillouin processing to microwave photonics," *Opt. Fiber Technol.*, vol. 8, no. 1, pp. 24–42, Jan. 2002.
[17] A. Loayssa and F. J. Lahoz, "Broad-band RF photonic phase shifter based on stimulated Brillouin scattering and single-sideband modulation," *IEEE Photon. Technol. Lett.*, vol. 18, no. 1, pp. 208–210, Jan. 1, 2006.
[18] W. Li, N. H. Zhu, and L. X. Wang, "Photonic phase shifter based on wavelength dependence of Brillouin frequency shift," *IEEE Photon. Technol. Lett.*, vol. 23, no. 14, pp. 1013–1015, Jul. 2011.